

# Topological directed amplification

Bikashkali Midya\*

Department of Physical Sciences, Indian Institute of Science Education and Research, Berhampur, India

A phenomenon of topological directed amplification of certain initial perturbations is theoretically revealed to emerge in a class of asymptotically stable skin-effect photonic lattices described by non-normal Toeplitz operators  $H_g$  with positive ‘numerical ordinate’  $\omega(H_g) > 0$ . Nonnormal temporal evolution, even in the presence of global dissipation, is shown to exhibit a counterintuitive transient phase of edge-state amplification—a behavior, drastically different from the asymptote, that spectral analysis of  $H_g$  fails to directly reveal. A consistent description of the effect is provided by the general tool of ‘pseudospectrum’, and a quantitative estimation of the maximum power amplification is provided by the *Kreiss constant*. A recipe to determine an optimal initial condition that will attain maximum amplification power is given by singular value decomposition of the propagator  $e^{-iH_g t}$ . Finally, it is predicted that the interplay between nonnormality and nonlinearity in a skin-effect laser array can exponentially enhance stable-emission power compared to a normal laser array.

## I. Introduction

Dynamical systems governed by Hamiltonians which fail to commute with their adjoints are called nonnormal in mathematical sense, and are in general extremely sensitive to boundary conditions. A class of such systems of enormous current interest is non-Hermitian topological lattices with nonreciprocal coupling<sup>1–3</sup>. One of the exotic features of these systems is the manifestation of non-Hermitian skin effect<sup>4–7</sup>, i.e. the localization of an arbitrary number of stationary states at one of the edges under open boundary conditions (OBC); whereas bulk states remain extended in a closed lattices under periodic boundary conditions (PBC). Origin of these localized skin modes is rooted in nontrivial topological winding of the bulk PBC spectral contour in complex-energy plane with respect to the interior OBC spectral points<sup>8–12</sup>. The interplay of topology, non-Hermiticity, and nonnormality is an active field of research both in theory<sup>15–46</sup> and experiments<sup>47–54</sup> with far reaching practical consequences.

An interesting question of fundamental importance is *how nonnormality influences the dynamical behavior of an injected power in a skin-effect lattice* remains largely unanswered. Here we uncover a peculiar phenomenon of topologically protected transient growth of initial energy directed towards an edge of a class of non-Hermitian skin-effect photonic lattices  $H_g$ . Such counterintuitive effect of directed amplification, although all modes decay monotonically, occurs due to an interplay between topological skin-effect and non-orthogonality of the eigenbasis of a nonnormal Hamiltonian governing the dynamics. While dominant imaginary part of the corresponding spectrum correctly predicts asymptotic decay dynamics, the same fails to explain more complex transient amplification phase. A consistent description of the effect is provided by the mathematical notion of pseudospectrum, defined by the union of spectra of a Hamiltonian under small perturbations. Use of pseudospectrum to deal nonnormality has a rich tradition in linear algebra<sup>55,56</sup>, its importance has been recognized in a variety of dynamical systems ranging from hydrodynamics<sup>57,58</sup>, and ecosystems<sup>59</sup>, optical

waveguides<sup>60</sup>, Lindblad master equation<sup>61</sup>, nonnormal networks<sup>62</sup>, to neuronal dynamics<sup>63</sup>. Due to extreme sensitivity of a Hamiltonian with strong nonnormality, a small perturbation can shift some of the pseudomodes into the upper-half of complex energy plane in favor of amplification. Remarkably, the amplification is topologically protected as long as corresponding pseudomodes, lying entirely inside the PBC spectral curve, are characterized by the underlying nontrivial topology of the system. Although a quantitative estimation of the maximum power amplification can be provided by the Kreiss matrix theorem<sup>55</sup>, a critical question is *what initial perturbations give rise to the maximum transient growth?* A systematic procedure based on singular value decomposition (SVD) of the propagator  $e^{-iH_g t}$  is explored here to reveal that an optimal initial condition that will attain maximum amplification is the principal right-singular vector. It is further predicted that the interplay between nonnormality and nonlinearity in a skin-effect laser array can exponentially enhance emission power compared to a normal laser array.

## II. Topological Hatano-Nelson lattice

To illustrate the phenomena, we consider a generic nonnormal photonic lattice given by the one-dimensional Hatano-Nelson model<sup>64</sup>. The system is described by a family of Hamiltonians  $H_g$  expressed in Toeplitz matrix form

$$[H_g]_{mn} = e^{-g}\delta_{m-1,n} + e^g\delta_{m+1,n} - i\gamma\delta_{m,n} \quad (1)$$

where  $e^{-g}$ ,  $e^g$ , and  $\gamma$  represent dimensionless nearest-neighbor forward-, backward-coupling amplitudes, and onsite loss, respectively. Parameters  $g$  and  $\gamma$  are real, and taken to be non-negative for definiteness. The commutator  $[H_g, H_g^\dagger] = 2\sinh 2g \text{diag}(1, 0, \dots, 0, -1)$  implies that the system is nonnormal for all  $g \neq 0$ , while nonnormality is absent in  $H_0$ . For a finite lattice with OBC,  $H_g$  for  $g \neq 0$  and  $g = 0$  are nonunitarily equivalent by a gauge transformation  $\vec{\Phi}_g = S\vec{\Phi}_0$ , with  $S_{mn} = e^{-gn}\delta_{m,n}$ , and  $\vec{\Phi}_g$  represents eigenvector of  $H_g$ . As a consequence, the OBC spectrum of  $H_{g \neq 0}$  is spectrally isomorphic to that of  $H_0$ :  $\sigma^{OBC} = \{2\cos \ell\pi/(N+1) - i\gamma : \ell = 1, 2, \dots, N\}$ , where  $N$  is

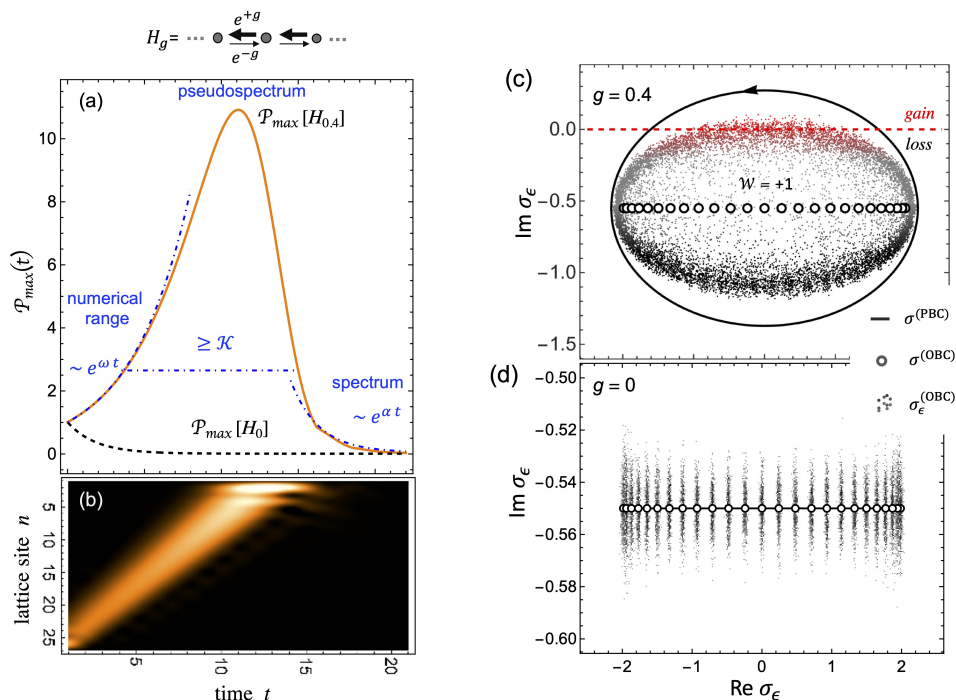


FIG. 1: (a) Magnitude of solutions of the dynamical Eq. (3) yielding maximum power is shown for a nonnormal lattice  $H_{0.4}$  and a normal lattice  $H_0$ . The behavior of transient amplification of power in a nonnormal lattice can be described by the information of numerical range and pseudospectrum of the Hamiltonian, while the asymptotic decay is given by the spectrum. A lower bound of the maximum power in the transient phase is given by the Kreiss constant  $\mathcal{K}(H_{0.4}) = 2.6$ . (b) The modal intensity dynamics of an initial condition which attains maximum power in the lattice  $H_{0.4}$  showing increase of power directed to the boundary where skin-modes localize. (c) The OBC, PBC spectrum, and  $\epsilon$ -pseudospectrum of  $H_{0.4}$  are shown for  $\epsilon \sim 0.15$ . Population of some pseudomodes (shown in red dots) in the gain region  $\text{Im } \sigma_\epsilon > 0$  originates from the center of unperturbed spectrum. Pseudomodes are protected by the nontrivial topological number  $\mathcal{W} = 1$ . (d) Pseudospectrum lies entirely in the lossy region  $\text{Im } \sigma_\epsilon < 0$  in the absence of nonnormality in  $H_0$ . Here  $N = 25$  and  $\gamma = 0.55$ .

the number of sites in a lattice. Components of stationary states  $\vec{\Phi}_g(E_\ell \in \sigma^{OBC})$  are given by  $\phi_{n,\ell} = e^{-gn} \sin \ell n \pi / (N + 1)$ ,  $n$  is the lattice site index, showing the exponential localization, i.e. skin-effect, of all states at the left edge of a lattice  $H_{g>0}$ . However, skin-modes are not necessarily orthogonal as a consequence of the nonunitary transformation. This has an intriguing implication, as will be elaborated below, that the evolution dynamics of  $H_g$  for  $g \neq 0$  is fundamentally different than that of  $g = 0$ ; a transient amplification phase exists in the former, while it never occurs in the later case. Topological origin of the skin-modes are related to the nontrivial winding number of the PBC spectra characterized by<sup>9,10</sup>

$$\mathcal{W}(z \in \sigma^{OBC}) = \int_0^{2\pi} \frac{dk}{2\pi i} \partial_k \log(\sigma^{PBC}(k) - z) \quad (2)$$

where PBC spectrum for  $g \neq 0$  lies on an ellipse  $\sigma^{PBC} = \{2 \cos(k - ig) - i\gamma : k \in [0, 2\pi]\}$ , and collapses to  $[-2 - i\gamma, 2 - i\gamma]$  when  $g = 0$ .  $\mathcal{W} = +1$  for  $g > 0$ , and 0 for  $g = 0$ . The index theorem of a Toeplitz operator<sup>65</sup> correlates analytical and topological index:  $\text{ind } H_g = -\mathcal{W}$ .

### III. Transient amplification

The phenomenon of transient amplification is analyzed after considering how an initial perturbation  $\vec{\Psi}_g(t = 0)$  evolves in a dissipative Hatano-Nelson lattice by the dynamical equation of motion

$$i\vec{\Psi}_g(t) = H_g \vec{\Psi}_g(t), \quad \|\vec{\Psi}_g(t = 0)\| = 1. \quad (3)$$

The general solution of Eq. (3) is given by  $\vec{\Psi}_g(t) = G(t)\vec{\Psi}_g(t = 0)$ , where  $G(t) = e^{-iH_g t}$  is the propagator. A physical observable of interest is the optical power determined by the Euclidean norm of the solution  $\mathcal{P}(t) = \|\vec{\Psi}_g(t)\| = (\sum_n |\psi_n(t)|^2)^{1/2}$  (square root of the actual power is considered for the convenient description of what follows henceforth), where  $\psi_n$ 's are modal amplitudes at site  $n$ .

*Amplification in a Hatano-Nelson Dimer.* As an example, we first consider a dimer amenable to analytical treatment. The eigenvalues and corresponding normalized eigenvectors of the dimer Hamiltonian

$$H_g = \begin{bmatrix} -i\gamma & e^g \\ e^{-g} & -i\gamma \end{bmatrix}, \quad (4)$$

are given by

$$E_{\pm} = \pm 1 - i\gamma, \quad \vec{\Phi}_g(E_{\pm}) = \frac{1}{\sqrt{e^{2g} + 1}} \begin{bmatrix} e^g \\ \pm 1 \end{bmatrix}. \quad (5)$$

Note that above eigenvectors are not orthogonal (with an exception for  $g = 0$ ) and approach each other in the large  $g$  limit. This is evident from following expression of the angle between two eigenvectors

$$\theta = \cos^{-1}(\tanh g) \rightarrow 0 \quad \text{as } g \rightarrow \infty. \quad (6)$$

Now consider time evolution of a specific initial state  $\vec{\Psi}_g(t \rightarrow 0) = [-i/\sqrt{2}, 1/\sqrt{2}]^T$ . The solution at a later time is given by  $\vec{\Psi}_g(t) \propto (i - e^g)e^{-iE_+t}\vec{\Phi}_g(E_+) + (i + e^g)e^{-iE_-t}\vec{\Phi}_g(E_-)$ . Even though the magnitude of solution eventually decays in time, it can initially grow due to non-orthogonal superposition of two eigenvectors that decay at different rates as time evolves. Corresponding time-dependent power

$$\begin{aligned} \mathcal{P}(t) &= e^{-\gamma t} (\cos^2 t + \cosh 2g \sin^2 t + \sinh g \sin 2t)^{\frac{1}{2}} \\ &\simeq 1 + (\sinh g - \gamma)t + \mathcal{O}(t^2) \quad \text{as } t \rightarrow 0, \end{aligned} \quad (7)$$

although decay for large time, but experiences initial amplification when  $\gamma < \sinh g$ .

*Amplification in a Hatano-Nelson lattice:* For a larger lattice, we first investigate maximum power that can be attained. Using the inequality  $\|AB\| \leq \|A\| \|B\|$ , we obtain maximum power:

$$\mathcal{P}_{\max}(t) = \sup_{\|\Psi_g(t=0)\|=1} \|G(t)\Psi_g(t=0)\| = \|G(t)\|, \quad (8)$$

given by the 2-norm, i.e. maximum singular value, of  $G(t)$  at each time  $t$ . Note that  $\mathcal{P}_{\max}(t)$  is different for different Hamiltonian  $H_g$ . For a given  $H_g$ ,  $\mathcal{P}_{\max}[H_g](t)$  represents an envelop of all possible power curves corresponding to the evolution of different initial conditions under  $H_g$ . Two particular examples of  $\mathcal{P}_{\max}$  are presented in Fig 1(a) corresponding to a nonnormal lattice ( $g = 0.4$ ) and a normal lattice ( $g = 0$ ), showing fundamentally different behaviors. Remarkable effect of short-time amplification phase, even in the presence of loss, is observed in the nonnormal lattice before the power decay asymptotically to zero. An intensity evolution pattern in  $H_{0.4}$  corresponding to an initial condition favoring maximum amplification is shown in Fig. 1(b); increased power unidirectionally evolves to the left edge of the lattice where skin-modes are localized. Note, however, that all skin-modes in general attenuate in a lattice with non-zero  $\gamma$ . Corresponding spectrum of the lattice, therefore, provides no information about the amplification phase. A complete description of the effect is given below by the notions of ‘numerical range’ and ‘pseudospectrum’, well known in matrix analysis<sup>55</sup>.

*Asymptotic phase,  $t \rightarrow \infty$ :* In this regime, the general solution of Eq. (3) reduces to  $\vec{\Psi}_g(t \rightarrow \infty) \sim e^{\alpha(H_g)t}$ , where  $\alpha(H_g)$  is the ‘spectral ordinate’<sup>66</sup> given by

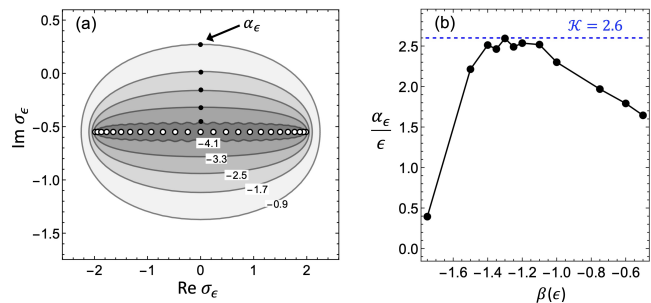


FIG. 2: (a) Pseudospectral ordinates  $\alpha_{\epsilon}(H_{0.4})$  are determined from the level curves  $\|(z - H_{0.4})^{-1}\| = 1/\epsilon$  shown here for different small perturbations  $\epsilon = 10^{\beta}$ , number on each contour represents a value of  $\beta$ . (b) Kreiss constant  $\mathcal{K}(H_{0.4}) \simeq 2.6$  is the maximum of  $\alpha_{\epsilon}/\epsilon \forall \epsilon \ll 1$ .

$\alpha = \sup \text{Im } \sigma^{OBC} = -\gamma$ , independent of the parameter  $g$ . This implies that solution and hence power decays to zero asymptotically whenever  $\gamma \neq 0, \forall g$ .

*Initial phase,  $t \rightarrow 0$ :* According to the Hille-Yoshida theorem<sup>55</sup>, the behavior of  $\mathcal{P}_{\max}$  is given by

$$\lim_{t \rightarrow 0} \frac{d}{dt} \mathcal{P}_{\max}[H_g](t) = \omega(H_g), \quad (9)$$

where  $\omega(H_g)$  is the ‘numerical ordinate’<sup>66</sup> defined by the maximum among imaginary parts of numerical range of  $H_g$ <sup>55,59,62</sup>, and determined analytically by

$$\omega = \sup \sigma^{OBC} \frac{[H_g - H_g^{\dagger}]}{2i} = 2 \sinh |g| \cos \frac{\pi}{N+1} - \gamma. \quad (10)$$

According to Eq. (9),  $\omega(H_g)$  is the slope of the curve  $\sim e^{\omega(H_g)t}$  which approximately fits  $\mathcal{P}_{\max}(t \rightarrow 0)$ . The result obtained in Eq. (10) is, therefore, key to predict the transient growth at the outset;  $\omega > 0$  implies the onset of energy growth, and negative value of  $\omega$  implies an opposite behavior. For  $H_0$ ,  $\omega(H_0) = -\gamma < 0$  implies that amplification is not possible in a dissipative lattice in the absence of nonnormality. Conversely, for a given  $\gamma \neq 0$ , it is always possible to find critical parameters ( $g, N$ ) for which  $\omega(H_g) > 0$ , indicating the possibility of amplification in a nonnormal lattice  $H_{g \neq 0}$ . For the example in Fig.1(a),  $\omega(H_{0.4}) = 0.82$ .

Eq. (10), further indicates that larger the values of  $g, N$ , and hence  $\omega$ , steeper the initial amplification. This is a direct consequence of the fact that deviation of  $H_g$  from the normality, measured by the Henrici’s departure from normality<sup>55,62</sup>:  $d(H_g) = \sqrt{\text{tr}(H_g^{\dagger} H_g - H_0^{\dagger} H_0)} = 2\sqrt{N-1} \sinh g$ , increases with either the nonreciprocal coupling parameter  $g$ , or/and the geometric dimension  $N$  of the lattice.

*Intermediate phase,  $t \rightarrow \text{finite}$ :* Having obtained the initial trend for the maximum power curve, we now describe the actual physics behind the amplification. Note that a nonnormal system are highly sensitive to perturbation. A convenient tool to investigate perturbed

system is the method of pseudospectrum. For  $\epsilon > 0$ , the  $\epsilon$ -pseudospectrum of  $H_g$  under OBC is defined by<sup>55</sup>  $\sigma_\epsilon^{OBC} = \{z \in \mathcal{C} : \|(z - H_g)^{-1}\| > \epsilon^{-1}\}$ . For efficient computation of pseudospectrum we consider collection of spectra of a perturbed Hamiltonian such that

$$\sigma_\epsilon^{OBC}(H_g) = \{z \in \mathcal{C} : z \in \sigma(H_g + H'), \|H'\| \leq \epsilon\}. \quad (11)$$

It has the properties that  $\sigma^{OBC} \subseteq \sigma_\epsilon^{OBC}$ ,  $\lim_{\epsilon \rightarrow 0} \sigma_\epsilon^{OBC} = \sigma^{OBC}$ , and  $\lim_{\epsilon \rightarrow 0, N \rightarrow \infty} \sigma_\epsilon^{OBC} = \sigma^{PBC}$ . Contrary to the normal system  $H_0$ , which is less sensitive to the perturbations and corresponding  $\epsilon$ -pseudospectrum lies within the  $\epsilon$ -neighborhood of the spectrum, perturbation to a nonnormal system  $H_{g \neq 0}$  yields drastic change in the spectrum. For  $H_g$  with sufficiently strong nonnormality, the corresponding unperturbed spectrum initially belongs to negative imaginary plane can protrude to the positive imaginary plane under small perturbation. This has the remarkable consequence that the dynamical evolution which, according to spectrum, must decay, but actually can grow upon perturbation by the pseudomodes with positive imaginary pseudo-eigenvalues. Refer to Fig. 1(c) for a particular example corresponding to the amplification shown in Fig. 1(a). Two important remarks are as follows. First, skin-modes which belongs to the center of the unperturbed spectrum becomes amplifying first. Second,  $\epsilon$ -pseudospectrum resides entirely inside the PBC spectrum for small enough  $\epsilon$ . According to Eq. (2), all the pseudomodes, therefore, satisfy  $\mathcal{W}(z \in \sigma_\epsilon^{OBC}) = +1$ . This implies that the effect of nonnormality induced transient growth is topologically protected.

Size of a maximum transient growth can be quantitatively estimated by the Kreiss matrix theorem<sup>55</sup>. In particular,  $\mathcal{K}(H_g) \leq \sup_t \mathcal{P}_{\max}[H_g](t) \leq eNK(H_g)$ , where the *Kreiss constant*  $\mathcal{K}$  is defined in terms of  $\epsilon$ -pseudospectral ordinate  $\alpha_\epsilon$  s.t.

$$\mathcal{K}(H_g) = \sup_{\epsilon > 0} \alpha_\epsilon(H_g)/\epsilon. \quad (12)$$

$\mathcal{K} > 1$  indicates that there must be amplification in the system. For the example in Fig 1(a),  $\mathcal{K}(H_{0.4}) = 2.6$  obtained from the pseudospectral level curves [see Fig. 2].

#### IV. Optimal initial condition for maximum amplification

Above analysis of  $\mathcal{P}_{\max}$  indicates that the transient growth of energy is possible in a nonnormal system. In practice, however, the size of amplification depends on particular form of an initial condition. Optimal initial perturbation that will reach maximum amplification  $\mathcal{P}_{\max}(t_*)$  at time  $t = t_*$  can be obtained by the method of singular value decomposition (SVD) of the propagator:  $G = U\Sigma V^\dagger$ , where diagonal entries  $\Sigma_{nn}$  are singular values, and corresponding normalized left- and right-singular vectors are given by the columns of the matrices  $U$  and  $V$ , respectively. If  $\Sigma_{11}$  denote the largest singular value of  $G(t_*)$ , then SVD implies that  $G\vec{v}_1 = \Sigma_{11}\vec{u}_1$ . This describes that  $G$  maps an initial vector  $\vec{v}_1$  to

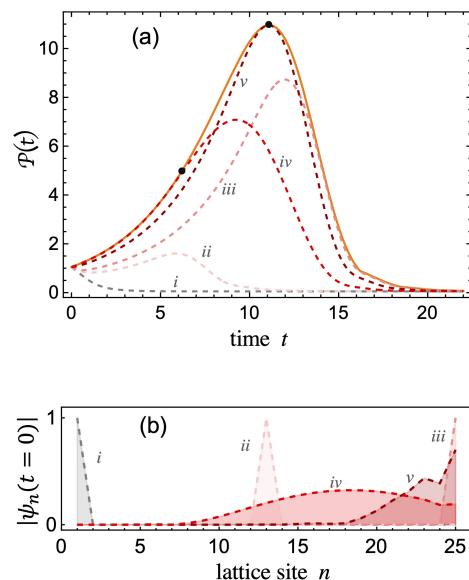


FIG. 3: (a) Transient dynamics of different initial conditions shown in (b) for a lattice  $H_{0.4}$ . ‘i’, ‘ii’, and ‘iii’ in (b) are single site excitations, while ‘iv’ and ‘v’ are obtained by SVD of the propagator  $e^{-iH_{0.4}t}$  at time  $t = 6$ , and  $t = 11$ , respectively. Solid line in (a) representing the envelop of  $\mathcal{P}_{\max}[H_{0.4}]$ . Optimal initial perturbation, marked as ‘v’ and ‘iv’, acquire maximum power amplifications shown by black dots at  $t = 11$  and  $t = 6$ , respectively.

an output vector  $\vec{u}_1$  amplified by  $\Sigma_{11} = \mathcal{P}_{\max}(t_*)$  [by Eq.(8)]. It is therefore instructive to consider  $\vec{v}_1$  as the initial condition for the Eq. (3) to achieve maximum amplification power at time  $t_*$ .

Above general idea is exemplified in Fig. 3 for  $H_g$  with  $g = 0.4$ . The initial conditions [marked as iv, v in the Fig. 3(b)] obtained by the SVD of  $G(t)$  at time  $t = 6$  and  $t = 11$  respectively, yields maximum amplification at the respective times. For comparison, single site excitation at three different locations of the lattice are also considered as initial conditions. It is seen that single site excitation away from the skin-mode localization center provides in general pretty good amplification. However, the excitation one at the left edge [marked as ‘i’ in Fig. 3(b)] does not amplify. Strictly speaking, *nonnormality of a lattice is not sufficient for observing transient amplification*, shape of initial profile is crucially important.

#### V. Nonnormal laser array

Finally, we briefly report the interplay between non-normality and nonlinearity in a coupled microring laser array. Array dynamics is determined by  $i\vec{\Psi} = (H_g + H_{NL})\vec{\Psi}$ , where

$$[H_{NL}]_{mn} = \frac{i\Gamma_n}{1 + |\psi_n|^2} \delta_{m,n} \quad (13)$$

with  $\Gamma_n$  represents site-dependent saturable gain<sup>67</sup>. In the absence of gain, passive skin-modes are localized at the left edge of a lattice with  $g > 0$  and only counter-

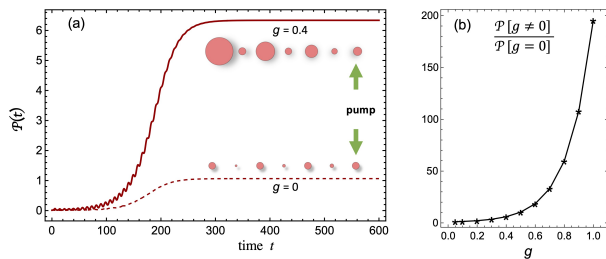


FIG. 4: (a) Emission powers of a array consisting  $N = 7$  lasers are shown for a nonnormal system  $g = 0.4$  and a normal lattice  $g = 0$ . In both cases,  $\gamma = 0.1$  and single site at the right edge is pumped with  $\Gamma_n = 0.5\delta_{n,7}$ . Absence of oscillation in power curve implies that the system is dynamically stable. Relative intensity distribution in individual lasers at time  $t=1000$  are shown by filled discs. (b) Ratio of average emission powers between a nonnormal and normal lattices vs the nonreciprocal coupling parameter  $g$  shows the exponential increment of power in the nonnormal array.

clockwise circulation in each of the rings is assumed. When gain is switched on by pumping only a single laser at the right edge (corresponds to the initial condition ‘iii’ for a linear lattice, see Fig. 4). This particular ‘nonlocal’ pumping strategy i.e. away from the lasing output, not

only convenient for practical implementation in experiment, but also is numerically verified to provide temporally stable emission (which is challenging to achieve in a large-scale laser array<sup>68</sup>). Total output power is seen to increase exponentially compared to a conventional laser array when degree of nonnormality is increased by tuning the coupling parameter  $g$  (elaborated in Fig. 4 with examples).

## VI. Conclusion

In summary, we have demonstrated that nonnormal nature of a class of recently-discovered topological skin-effect lattice can give rise to a fundamentally new effect of topologically-protected one-way transient amplification of injected energy. Condition of amplification is analytically derived, bounds of maximum amplification, and optimal initial condition to attain it are determined by the pseudospectrum of the Hamiltonian, and SVD of the propagator, respectively. Potential of exponential enhancement of emission power is revealed in a nonnormal laser array. Reported results on nonnormal wave dynamics can be tested in quantum and classical topological devices with engineered nonnormality, particularly for sensing weak signals, and large-scale high-power laser applications.

\* Electronic address: [midya@iiserbpr.ac.in](mailto:midya@iiserbpr.ac.in)

- <sup>1</sup> E. J. Bergholtz, J. C. Budich, F. K. Kunst, Exceptional Topology of Non-Hermitian Systems, *Rev. Mod. Phys.* 93, 15005 (2021).
- <sup>2</sup> X. Zhang, T. Zhang, M.-H. Lu, Y.-F. Chen, A review on non-Hermitian skin effect, arXiv: 2205.08037 (2022).
- <sup>3</sup> N. Okuma, M. Sato, Non-Hermitian topological phenomena: A review, arXiv: 2205.10379 (2022).
- <sup>4</sup> S. Yao and Z. Wang, Edge States and Topological Invariants of Non-Hermitian Systems, *Phys. Rev. Lett.* 121, 086803 (2018).
- <sup>5</sup> T. E. Lee, Anomalous edge state in a non-hermitian lattice, *Phys. Rev. Lett.* 116, 133903 (2016).
- <sup>6</sup> C.H. Lee and R. Thomale, Anatomy of skin modes and topology in non-Hermitian systems, *Phys. Rev. B* 99, 201103(R) (2019).
- <sup>7</sup> V. M. Martinez Alvarez, J. E. Barrios Vargas, and L. E. F. Foa Torres, Non-Hermitian robust edge states in one dimension: Anomalous localization and eigenspace condensation at exceptional points, *Phys. Rev. B* 97, 121401(R) (2018).
- <sup>8</sup> D.S. Borgnia, A.J. Kruchkov, and R.-J. Slager, Non-Hermitian Boundary Modes and Topology, *Phys. Rev. Lett.* 124, 056802 (2020).
- <sup>9</sup> N. Okuma, K. Kawabata, K. Shiozaki, and M. Sato, Topological Origin of Non-Hermitian Skin Effects, *Phys. Rev. Lett.* 124, 086801 (2020).
- <sup>10</sup> Z. Gong, Y. Ashida, K. Kawabata, K. Takasan, S. Higashikawa, M. Ueda, Topological Phases of Non-Hermitian Systems. *Phys. Rev. X* 8, 031079 (2018).
- <sup>11</sup> K. Wang, A. Dutt, K. Y. Yang, C.C. Wojcik, J. Vuckovic, and S. Fan, Generating arbitrary topological windings of a non-Hermitian band, *Science* 371, 1240 (2021).

- <sup>12</sup> K. Zhang, Z. Yang, and C. Fang, Correspondence between Winding Numbers and Skin Modes in Non-Hermitian Systems, *Phys. Rev. Lett.* 125, 126402 (2020).
- <sup>13</sup> C. H. Lee, L. Li, and J. Gong, Hybrid Higher-Order Skin-Topological Modes in Non-reciprocal Systems, *Phys. Rev. Lett.* 123, 016805 (2019).
- <sup>14</sup> K. Kawabata, K. Shiozaki, M. Ueda, and M. Sato, Symmetry and Topology in Non-Hermitian Physics, *Phys. Rev. X* 9, 041015 (2019).
- <sup>15</sup> F. Song, S. Yao, and Z. Wang, Non-Hermitian skin effect and chiral damping in open quantum systems, *Phys. Rev. Lett.* 123, 170401 (2019).
- <sup>16</sup> W.-T. Xue, Y.-M. Hu, F. Song, and Z. Wang, Non-Hermitian Edge Burst, *Phys. Rev. Lett.* 128, 120401 (2022).
- <sup>17</sup> S. Lieu, Topological phases in the non-Hermitian Su-Schrieffer-Heeger model, *Phys. Rev. B* 97, 045106 (2018).
- <sup>18</sup> K. Yokomizo and S. Murakami, “Non-Bloch Band Theory of Non-Hermitian Systems,” *Phys. Rev. Lett.* 123, 066404 (2019).
- <sup>19</sup> M. Ezawa, Non-Hermitian boundary and interface states in nonreciprocal higher-order topological metals and electrical circuits, *Phys. Rev. B* 99, 121411(R) (2019).
- <sup>20</sup> L. Herviou, J.H. Bardarson, and N. Regnault, Defining a bulk-edge correspondence for non-Hermitian Hamiltonians via singular-value decomposition, *Phys. Rev. A* 99, 052118 (2019).
- <sup>21</sup> B. Midya, H. Zhao, and L. Feng, Non-hermitian photonics promises exceptional topology of light, *Nat. Commun.* 9, 1-4 (2018).
- <sup>22</sup> S. Longhi, Self-healing of non-Hermitian topological skin modes, *Phys. Rev. Lett.* 128, 157601 (2022).
- <sup>23</sup> S. Longhi, Non-Bloch-Band Collapse and Chiral Zener

- Tunneling, Phys. Rev. Lett. 124, 066602 (2020).
- 24 S. Longhi, Topological phase transition in non-Hermitian quasicrystals, Phys. Rev. Lett. 122, 237601 (2019).
  - 25 S. Longhi, Non-Hermitian Gauged Topological Laser Arrays, Ann. Phys. 530, 1800023 (2018).
  - 26 W. X. Teo, W. Zhu, and J. Gong, Tunable two-dimensional laser arrays with zero-phase locking, Phys. Rev. B 105, L201402 (2022).
  - 27 B. Zhu, Q. Wang, D. Leykam, H. Xue, Q. J. Wang, and Y. D. Chong, Anomalous single-mode lasing induced by nonlinearity and the non-Hermitian skin effect, to appear in Phys. Rev. Lett. (2022).
  - 28 C. C. Wanjura, M. Brunelli, and A. Nunnenkamp, Topological framework for directional amplification in driven-dissipative cavity arrays, Nat. Commun. 11, 3149 (2020).
  - 29 C.-X. Guo, C.-H. Liu, X.-M. Zhao, Y. Liu, and S. Chen, Exact Solution of Non-Hermitian Systems with Generalized Boundary Conditions: Size-Dependent Boundary Effect and Fragility of the Skin Effect, Phys. Rev. Lett. 127, 116801 (2021).
  - 30 J. Y. Lee, J. Ahn, H. Zhou, and A. Vishwanath, Topological Correspondence between Hermitian and Non-Hermitian Systems: Anomalous Dynamics, Phys. Rev. Lett. 123, 206404 (2019).
  - 31 N. Okuma and M. Sato, Non-Hermitian Skin Effects in Hermitian Correlated or Disordered Systems: Quantities Sensitive or Insensitive to Boundary Effects and Pseudo-Quantum-Number, Phys. Rev. Lett. 126, 176601 (2021).
  - 32 H. Schomerus, Nonreciprocal response theory of non-Hermitian mechanical metamaterials: Response phase transition from the skin effect of zero modes, Phys. Rev. Research 2, 013058 (2020).
  - 33 G. G. Pyrialakos, H. Ren, P. S. Jung, M. Khajavikhan, and D. N. Christodoulides, Thermalization Dynamics of Nonlinear Non-Hermitian Optical Lattices, Phys. Rev. Lett. 128, 213901 (2022).
  - 34 H.-G. Zirnstein, G. Refael, and B. Rosenow, Bulk-Boundary Correspondence for Non-Hermitian Hamiltonians via Green Functions, Phys. Rev. Lett. 126, 216407 (2021).
  - 35 T. Haga, M. Nakagawa, R. Hamazaki, and M. Ueda, Liouvillean Skin Effect: Slowing Down of Relaxation Processes without Gap Closing, Phys. Rev. Lett. 127, 070402 (2021).
  - 36 N. Okuma and M. Sato, Quantum anomaly, non-Hermitian skin effects, and entanglement entropy in open systems, Phys. Rev. B 103, 085428 (2021).
  - 37 L. Li, C. H. Lee, S. Mu, J. Gong, Critical non-Hermitian skin effect, Nat. Commun. 11, 5491 (2020).
  - 38 D. A. Zezyulin, Y. V. Kartashov, and Vladimir V. Konotop, Superexponential amplification, power blowup, and solitons sustained by non-Hermitian gauge potentials, Phys. Rev. A 104, L051502 (2021).
  - 39 J. Claes and T.L. Hughes, Skin effect and winding number in disordered non-Hermitian systems, Phys. Rev. B 103, L140201 (2021).
  - 40 A. McDonald and A. A. Clerk, Exponentially-enhanced quantum sensing with non-Hermitian lattice dynamics, Nat. Commun. 11, 5382 (2020).
  - 41 C. Scheibner, W. T. M. Irvine, and V. Vitelli, "Non-Hermitian Band Topology and Skin Modes in Active Elastic Media," Phys. Rev. Lett. 125, 118001 (2020).
  - 42 T. Yoshida, T. Mizoguchi, and Y. Hatsugai, Mirror skin effect and its electric circuit simulation, Phys. Rev. Research 2, 022062 (2020).
  - 43 C. C. Wojcik, X.-Q. Sun, T. Bzdusek, and S. Fan, Homotopy characterization of non-Hermitian Hamiltonians, Phys. Rev. B 101, 205417 (2020).
  - 44 S. Longhi, D. Gatti, and G. D. Valle, Non-Hermitian transparency and one-way transport in low-dimensional lattices by an imaginary gauge field, Phys. Rev. B 92, 094204 (2015).
  - 45 L. Li, C. H. Lee, and J. Gong, Topological switch for non-Hermitian skin effect in cold-atom systems with loss. Phys. Rev. Lett. 124, 250402 (2020).
  - 46 Y. Song, W. Liu, L. Zheng, Y. Zhang, B. Wang, and P. Lu, Two-dimensional non-Hermitian Skin Effect in a Synthetic Photonic Lattice, Phys. Rev. Applied 14, 0604076 (2020).
  - 47 L. Xiao, T. Deng, K. Wang, G. Zhu, Z. Wang, W. Yi, and P. Xue, "Non-Hermitian bulk-boundary correspondence in quantum dynamics," Nat. Phys. 16, 761 (2020).
  - 48 A. Ghatak, M. Brandenbourger, J. van Wezel, C. Coullais, Observation of non-Hermitian topology and its bulk-edge correspondence, Proc Nat. Acad. Sci. 117, 29561 (2020).
  - 49 M. Brandenbourger, X. Locsin, E. Lerner, and C. Coullais, Non-reciprocal robotic metamaterials, Nat. Commun. 10, 4608 (2019).
  - 50 Gou et al., Tunable non-reciprocal quantum transport through a dissipative aharonov-bohm ring in ultracold atoms. Phys. Rev. Lett. 124, 070402 (2020).
  - 51 Z. Lin, L. Ding, S. Ke, and X. Li, Steering non-Hermitian skin modes by synthetic gauge fields in optical ring resonators, Opt. Lett. 46, 3512 (2021).
  - 52 L. Zhang et. al., Acoustic non-Hermitian skin effect from twisted winding topology, Nat. Commun. 12, 6297 (2021).
  - 53 S. Weidemann, M. Kremer, T. Helbig, T. Hofmann, A. Stegmaier, M. Greiter, R. Thomale, and A. Szameit, "Topological funneling of light, Science 368, 311 (2020).
  - 54 T. Helbig, T. Hofmann, S. Imhof, M. Abdelghany, T. Kiessling, L. W. Molenkamp, C. H. Lee, A. Szameit, M. Greiter, R. Thomale, Generalized bulk-boundary correspondence in non-Hermitian topoelectrical circuits, Nat. Phys. 16, 747 (2020).
  - 55 L. N. Trefethen and M. Embree, Spectra and Pseudospectra, Princeton University Press (2005).
  - 56 A. Böttcher and S. M. Grudsky, Spectral Properties of Banded Toeplitz Matrices., SIAM (2005).
  - 57 L.N.Trefethen, A.E.Trefethen,S.C.Reddy,T.A.Driscoll, Hydrodynamic stability without eigenvalues, Science 261, 578– 584 (1993).
  - 58 S. C. Reddy, P. J. Schmid, D. S. Henningson, Pseudospectra of the orr-sommerfeld operator, SIAM J. Appl. Math.53, 15–47 (1993).
  - 59 M. G. Neubert, and H. Caswell, Alternatives to Resilience for Measuring the Responses of Ecological Systems to Perturbations, Ecology 78, 653-665 (1997).
  - 60 K.G.Makris, L.Ge, H.E.Türeci, Anomalous transient amplification of waves in non-normal photonic media,Phys.Rev.X 4, 041044 (2014).
  - 61 N. Okuma, and Y. O. Nakagawa, Non-normal Hamiltonian dynamics in quantum systems and its realization on quantum computers, Phys. Rev. B 105, 054304 (2022).
  - 62 M. Asllani, R. Lambiotte, T. Carletti, Structure and dynamical behavior of non-normal networks, Sci. Adv. 4, eaau9403 (2018).
  - 63 B. K. Murphy, K. D. Miller, Balanced amplification: A new mechanism of selective amplification of neural activity patterns, Neuron 61, 635–648 (2009).
  - 64 N. Hatano and D.R. Nelson, Localization Transitions in Non-Hermitian Quantum Mechanics, Phys. Rev. Lett. 77, 570 (1996).
  - 65 L. B. de Monvel, On the Index of Toeplitz Operators of

Several Complex Variables, *Inventiones math.* 50, 249-272 (1979).

- <sup>66</sup> The terminology of ‘spectral ordinate’ is coined here to refer the largest imaginary part of a complex energy spectrum, in contrast to ‘spectral abscissa’ which refers to the largest real part. Same argument is valid for the nomenclature of ‘numerical ordinate’.
- <sup>67</sup> G. Harari et al. Topological insulator laser: theory, *Science* 359, eaar4003 (2018).
- <sup>68</sup> S. Longhi and L. Feng, Mitigation of dynamical instabilities in laser arrays via non-Hermitian coupling, *APL Photonics* 3, 060802 (2018).